# Hybrid Breakdown Caused by Substitution of the X Chromosome Between Two Mouse Subspecies

**Ayako Oka,*,† Akihiko Mita,* Noriko Sakurai-Yamatani,* Hiromi Yamamoto,* Nobuo Takagi,‡ Toshiyuki Takano-Shimizu,§ Kiyotaka Toshimori,** Kazuo Moriwaki†† and Toshihiko Shiroishi*,†,[1]**

**Mammalian Genetics Laboratory, National Institute of Genetics, Mishima, Shizuoka-ken 411-8540, Japan, †Graduate University for Advanced Studies, Hayama, Kanagawa-ken 240-0193, Japan, ‡Division of Bioscience, Graduate School of Environmental Earth Science, Hokkaido University, Kita-ku, Sapporo 060-0810, Japan, §Department of Population Genetics, National Institute of Genetics, Mishima, Shizuoka-ken 411-8540, Japan, **Department of Anatomy and Developmental Biology (G1), Graduate School of Medicine, Chiba University, Chiba City, 260-8670, Japan and ††RIKEN BioResource Center, Tsukuba, Ibaraki 305-0074, Japan*

Manuscript received May 28, 2003
Accepted for publication November 2, 2003

ABSTRACT

Hybrid breakdown is a type of reproductive failure that appears after the $F_2$ generation of crosses between different species or subspecies. It is caused by incompatibility between interacting genes. Genetic analysis of hybrid breakdown, particularly in higher animals, has been hampered by its complex nature (*i.e.*, it involves more than two genes, and the phenotype is recessive). We studied hybrid breakdown using a new consomic strain, C57BL/6J-$X^{MSM}$, in which the X chromosome of C57BL/6J (derived mostly from *Mus musculus domesticus*) is substituted by the X chromosome of the MSM/Ms strain (*M. m. molossinus*). Males of this consomic strain are sterile, whereas $F_1$ hybrids between C57BL/6J and MSM/Ms are completely fertile. The C57BL/6J-$X^{MSM}$ males showed reduced testis weight with variable defects in spermatogenesis and abnormal sperm head morphology. We conducted quantitative trait locus (QTL) analysis for these traits to map the X-linked genetic factors responsible for the sterility. This analysis successfully detected at least three distinct loci for the sperm head morphology and one for the testis weight. This study revealed that incompatibility of interactions of X-linked gene(s) with autosomal and/or Y-linked gene(s) causes the hybrid breakdown between the genetically distant C57BL/6J and MSM/Ms strains.

HYBRIDS between individuals of two genetically diverged populations show different extents of reproductive failure; this failure is known as reproductive isolation. This reduction of fecundity of the hybrids prevents gene flow across the two different populations, accelerating genetic differentiation and eventually contributing to speciation. Thus, the study of reproductive isolation is essential for understanding the process of speciation.

In mice, genetic studies on reproductive isolation have focused mostly on male sterility in $F_1$ hybrids between subspecies or closely related species. This hybrid sterility is likely caused by interallelic incompatibility at a given locus or at several different loci. In such cases, one allele or a set of alleles is fixed or predominates in each genetically differentiating population. Hybrid sterility has been observed in male offspring of crosses between different subspecies (Forejt and Ivanyi 1975; Forejt *et al.* 1991; Trachtulec *et al.* 1997) and between different species (Guénet *et al.* 1990; Pilder *et al.* 1991, 1993, 1997; Pilder 1997; Elliott *et al.* 2001).

Hybrid breakdown is another type of reproductive isolation, defined as inviability or sterility observed only in the $F_2$ or later generations of interspecific or intersubspecific crosses, while $F_1$ hybrids are viable and fully fertile. Hybrid breakdown may be due to disruption of interaction of genes at different loci as the genes segregate after the $F_1$ generation. Assuming that two diverging populations have different alleles at each of two loci that genetically interact, it is inferred that the proper interaction may occur only in the allele combinations that occur in each of the two diverging populations. Hybrid breakdown is thus hypothesized to arise when genetic segregation causes alleles of each interacting locus to become homozygous in an improper way. Therefore, the hybrid breakdown appears as a recessive trait (Muller 1940; Orr 1993). Little is known about the genetic basis of hybrid breakdown, because it is both recessive and complex, involving more than two genes; these characteristics may impede genetic analysis.

MSM/Ms is a mouse strain derived from the Japanese wild mouse, *Mus musculus molossinus*. It and a Western European subspecies, *Mus musculus domesticus*, diverged from a common ancestor ~1 million years ago (Moriwaki 1994). The $F_1$ hybrid males of the MSM/Ms and standard inbred strains, the genome of which mostly originated from *M. m. domesticus* (Bonhomme *et al.* 1987;

[1]*Corresponding author:* Mammalian Genetics Laboratory, National Institute of Genetics, Yata 1111, Mishima, Shizuoka-ken 411-8540, Japan. E-mail: tshirois@lab.nig.ac.jp

Moriwaki 1994), are fully fertile. Successive inbreeding of the hybrids, however, gradually reduced fecundity, suggesting that genetic segregation of the two mouse genomes causes hybrid breakdown (K. Moriwaki and T. Shiroishi, unpublished data). A role for the X chromosome in this hybrid incompatibility was suggested in a study of hybrids between MSM/Ms and XO females that carry a hemizygous X chromosome in the hybrid background of C57BL/6J and CBA strains. Since no homologous recombination occurs through the whole X chromosome in XO females, this breeding scheme allowed introduction of the MSM/Ms-derived X chromosome as a whole into the C57BL/6J/CBA hybrid background. Through successive generations of backcrossing to the standard strain, male fecundity was reduced and abnormal spermatozoa appeared (Takagi *et al.* 1994).

Currently, we are generating a series of consomic strains using two mouse strains, MSM/Ms and C57BL/6J. In consomic strains, one chromosome of a recipient strain is replaced as a whole by the same chromosome from a donor strain, leaving the rest of the recipient strain's chromosomes intact (Nadeau *et al.* 2000). As the mouse has 19 autosomes and two sex chromosomes, X and Y, we introduce all 21 chromosomes of the MSM/Ms strain into the genetic background of the C57BL/6J strain (Figure 1). This full set of consomic strains will cover the whole genome of the donor strain MSM/Ms, and it enables mapping of gene(s) responsible for phenotypes that differ between the MSM/Ms and C57BL/6J strains. During the process of generating the consomic strains, we have noticed that males of the X chromosomal consomic strain, in which the X chromosome of the C57BL/6J strain is substituted by its counterpart from the MSM/Ms strain, showed reduced fecundity. This reduction became pronounced in the third and subsequent backcross generations. This finding confirmed that the X chromosome is involved in the hybrid breakdown.

To clarify the genetic basis of the hybrid breakdown involving the X chromosome, we carried out in-depth characterization of reproductive phenotypes of the X chromosomal consomic males at different backcross generations. Quantitative trait locus (QTL) analysis to map the X-linked genes responsible for the loss of fecundity successfully detected distinct QTL. Thus, study of the genetic basis of the hybrid breakdown using an X chromosomal consomic strain appears to provide new insight into genome differentiation and reproductive isolation during speciation.

## MATERIALS AND METHODS

**Animals:** The C57BL/6J strain was purchased in 1984 from the Jackson Laboratory (Bar Harbor, ME) and has been maintained in the animal facility at the National Institute of Genetics (NIG; Mishima, Japan). The MSM/Ms strain, which was derived from the Japanese wild mouse, *M. m. molossinus*, was established and maintained at NIG (Moriwaki 1994; Bonhomme and Guénet 1996). To construct the X chromosomal consomic strain, (C57BL/6J × MSM/Ms) $F_1$ females were backcrossed to C57BL/6J males for 10 generations (Figure 1). In each backcross generation, females heterozygous for nonrecombinant X chromosomes of the MSM/Ms strain were selected by genotyping for microsatellite markers across the X chromosome and then mated with C57BL/6J males.

**Genotyping of the X chromosome markers:** The following MIT microsatellite markers, which differ between the C57BL/6J and the MSM/Ms strains, were monitored during the construction of the consomic strain: *DXMit89*, *DXMit72*, *DXMit50*, *DXMit109*, *DXMit147*, *DXMit95*, *DXMit97*, *DXMit217*, *DXMit249*, and *DXMit160*, which are located at 3.0, 4.8, 14.1, 27.0, 33.5, 43.0, 49.0, 63.0, 70.5, and 73.3 cM, respectively, from the centromere. PCR primers for the above markers were purchased from Research Genetics (Huntsville, AL) or were ordered from RIKAKEN (Nagoya, Japan) or Sawaday Technology (Tokyo), using information from the Whitehead Institute/MIT Genome Database (http://www-genome.wi.mit.edu/). Information on length polymorphisms of the microsatellite markers was obtained from the Mouse Microsatellite Database of Japan (MMDBJ, http://www.shigen.nig.ac.jp/mouse/mmdbj/mouse.html). Genomic DNA for genotyping was prepared from ear or liver. The PCR-amplified DNA was separated by electrophoresis on agarose gels and stained with ethidium bromide.

**Analysis of male fecundity:** For evaluation of male fecundity in natural mating, males were premated with a C57BL/6J female for replacement of old spermatozoa in the epididymides and stimulation of spermatogenesis. Approximately 10 days after premating, an individual male of 3–4 months was caged for 10 days with three 2- to 3-month-old C57BL/6J females, and then they were separated. These females were dissected after an additional 10 days, and any embryos were counted. For analysis of fertilization *in vivo*, 2-month-old C57BL/6J females were superovulated by intraperitoneal injection of 5 units pregnant mare serum gonadotropin (Teikoku Hormone, Tokyo), followed 46–48 hr later by 5 units human chorionic gonadotropin (Teikoku Hormone), and then the females were mated with a 3- to 4-month-old male. Females with copulatory plugs were dissected to collect oocytes and/or embryos from the oviducts on the day after the copulation. Oocytes/embryos were flushed from the oviducts with Whittingham's medium (Whittingham *et al.* 1972).

**Histology of testis:** Three- to 4-month-old males were dissected, and pairs of the testes were weighed. The testes and epididymides were placed in fresh Bouin's fixative at room temperature. Excess fixative was removed with 70% ethanol. Tissues were then dehydrated and embedded in paraffin for microtome sections. The sections (6 μm) were stained with hematoxylin and eosin. To evaluate testosterone levels, serum samples were assayed at SRL (Tokyo), using Coat-A-Count kits (Diagnostic Products, Los Angeles) according to the manufacturer's instructions.

**Morphological analysis of spermatozoa:** For morphological analysis, spermatozoa were obtained from cauda epididymides and were observed under a phase contrast microscope. For transmission electron microscopy (TEM), testes were fixed by perfusion via the left ventricle with 2.5% glutaraldehyde in 0.1 M cacodylate buffer. The removed testes were further immersed for 2 hr in the same fixative, washed thoroughly, and then cut into small pieces. The small pieces were fixed with 2% osmium tetroxide, routinely dehydrated, and embedded in Epon 812 (Toshimori and Oura 1993). Ultrathin sections were made with a diamond knife on an ultratome (LKB model 2088; LKB-Producter AB, Bromma, Sweden) and double

stained with uranium acetate and lead citrate in an autostainer (LKB model 2168). Observation was done under a transmission electron microscope at 75 kV accelerating voltage (H7100 type; Hitachi, Japan).

**Acrosome reaction:** For assessment of the acrosome reaction and sperm motility, spermatozoa were collected from the cauda epididymides, dispersed into a 300-μl drop of Toyoda-Yokoyama-Hoshi (TYH) medium (Toyoda *et al.* 1971) under paraffin oil, and incubated at 37° in 5% $CO_2$. To evaluate the acrosome reaction, numbers of spermatozoa were adjusted to $\sim 1 \times 10^6$/ml, and then the calcium ionophore A23187 (Sigma, St. Louis) was added to 10 μM. At time zero and at 1 and 2 hr, sperm samples (50 μl) were fixed by 100 μl of 4% paraformaldehyde for 10 min at room temperature. Spermatozoa were twice collected by centrifugation and resuspended in 100 μl of 0.1 M ammonium acetate (pH 9.0). Aliquots (10 μl) of the final sperm suspension were dried onto glass slides. Dried spermatozoa were stained for 2 min with 0.22% Coomassie brilliant blue R250 (Fluka Chemie AG, Buchs, Switzerland) in 50% methanol/10% glacial acetic acid, rinsed with water, and mounted. The acrosome-reacted sperm were counted under a light microscope by the loss of intense staining on the anterior aspect of the sperm head. More than 200 spermatozoa from each individual were counted.

**Assay for sperm motility:** The sperm motility index (SMI) was measured by a sperm quality analyzer-SQAII C (Medical Electronic Systems, Caesarea, Israel) at 1, 2, 3, and 4 hr after incubation in TYH medium. Spermatozoa were counted with a hemocytometer, and SMI values standardized with the number of spermatozoa, $10^7$/ml, were used for the evaluation. To examine sperm transport in the female reproductive tract, males were mated with superovulated females. Five hours after mating, spermatozoa from uteri were dispersed in TYH medium and collected by centrifugation. Spermatozoa from oviducts were flushed with TYH medium and collected by centrifugation.

**Classification of shape of sperm head for QTL analysis:** Spermatozoa from cauda epididymides were stained with 2% trypan blue (E. Merck, Darmstadt, Germany) and Giemsa's stain solution (E. Merck) as described (Didion *et al.* 1989). More than 100 spermatozoa from each individual were observed under a light microscope and classified into the six types as described in Figure 4.

**QTL analysis:** In total, 179 male progeny of the backcross generations $N_{5-7}$ were used for QTL analysis. The following microsatellite markers were used in this analysis in addition to the 10 microsatellite markers described above: *DXMit166*, *DXMit193*, *DXMit144*, and *DXMit4*. Composite interval mapping was used to localize QTL governing testis weight and sperm head morphology, using model 6 of the Zmapqtl program in QTL Cartographer software (http://statgen.ncsu.edu/qtlcart/cartographer.html; Basten *et al.* 1997). Composite interval mapping combines classical interval mapping with multiple regressions, allowing more precise QTL localization than does classical interval mapping. Additionally, composite interval mapping controls for spurious ghost loci (Zeng 1993, 1994). Background markers for composite interval mapping were chosen using the SRmapqtl module of QTL Cartographer. Composite interval mapping was performed using 1-cM increments with a window size of 10 cM. QTL cartographer provides the likelihood-ratio test statistic for testing and estimating additive and dominance effects of a QTL. Because X-linked traits were analyzed in males, the dominance effect of a QTL could not be estimated. The hypotheses for testing are $H_0$, no QTL effect at the tested position, namely $a = 0$ (where $a$ is the additive effect of a putative QTL), and $H_1$, a QTL effect at the tested position, namely $a = 0$. The likelihood test statistic is $-2 \ln(L_0/L_1)$, where $L_0$ is the maximum likelihood under the null hypothesis $H_0$, and $L_1$ is the maximum likelihood under the alternative hypotheses $H_1$. The likelihood-ratio test statistic = 2 × (ln 10) × LOD (= 4.61 × LOD). The 5% critical value may be taken as $\chi^2_{0.05/12=0.0042} = 11.0$ when d.f. = 2.

## RESULTS

**Reduced fecundity of B6-X$^{MSM}$Y males:** To construct the X chromosomal consomic strain, we backcrossed (C57BL/6J × MSM/Ms) $F_1$ females to C57BL/6J males beyond 10 generations (Figure 1). In each backcross generation, females carrying a nonrecombinant X chromosome of the MSM/Ms strain were selected and mated with C57BL/6J males for the next generation. Hereafter, we refer to the males with a nonrecombinant MSM/Ms-derived X chromosome after the first backcross generation as B6-X$^{MSM}$Y and to the males from the same litter with a nonrecombinant C57BL/6J-derived X chromosome as B6-X$^{B6}$Y.

The fertility of (C57BL/6J × MSM/Ms) $F_1$ hybrids and of the B6-X$^{MSM}$Y males was examined by caging each male with three C57BL/6J females for 10 days. The $F_1$ males were mostly fertile, and they sired litters as large as those sired by the control C57BL/6J males (Table 1). At the first backcross generation, $N_2$, B6-X$^{MSM}$Y males were almost fertile, but the average litter size was somewhat reduced. The males of the next backcross generation, $N_3$, exhibited markedly reduced fecundity. Only 2 of 10 males were judged to be fertile, and both the frequency of pregnant females and the litter size decreased significantly. After 8–10 generations of backcrossing ($N_{8-10}$), all the B6-X$^{MSM}$Y males were completely sterile. In contrast, the B6-X$^{B6}$Y males of the same generations showed full fecundity. All females heterozygous for the X chromosome, B6-X$^{MSM}$X$^{B6}$, were fertile during all the backcross generations (data not shown).

To reveal the cause of the sterility, we recovered oocytes and/or embryos from the oviducts of C57BL/6J females on the day after copulation with the B6-X$^{MSM}$Y males. Eight out of 24 B6-X$^{MSM}$Y males of the $N_{7-9}$ produced copulation plugs. This rate was not significantly lower than that observed in the B6-X$^{B6}$Y males (data not shown). In contrast, no two-cell-stage embryos were recovered from the crosses with the B6-X$^{MSM}$Y males, a significant reduction compared to the number of two-cell-stage embryos recovered from the crosses with the B6-X$^{B6}$Y males (Table 2).

**Reduced testis weight and abnormal testicular histology in B6-X$^{MSM}$Y males:** Average body weight of (C57BL/6J × MSM/Ms) $F_1$ males (26.9 g ± 2.4, $n = 3$) was similar to that of the C57BL/6J strain. The testis weight of the $F_1$ males (66.1 mg ± 13.4, $n = 4$) was smaller than that of the C57BL/6J, but the spermatogenesis of the $F_1$ males appeared normal (data not shown). Average body weight of the B6-X$^{MSM}$Y males of the $N_{5-7}$ was similar to that of their B6-X$^{B6}$Y littermates (Table 3).

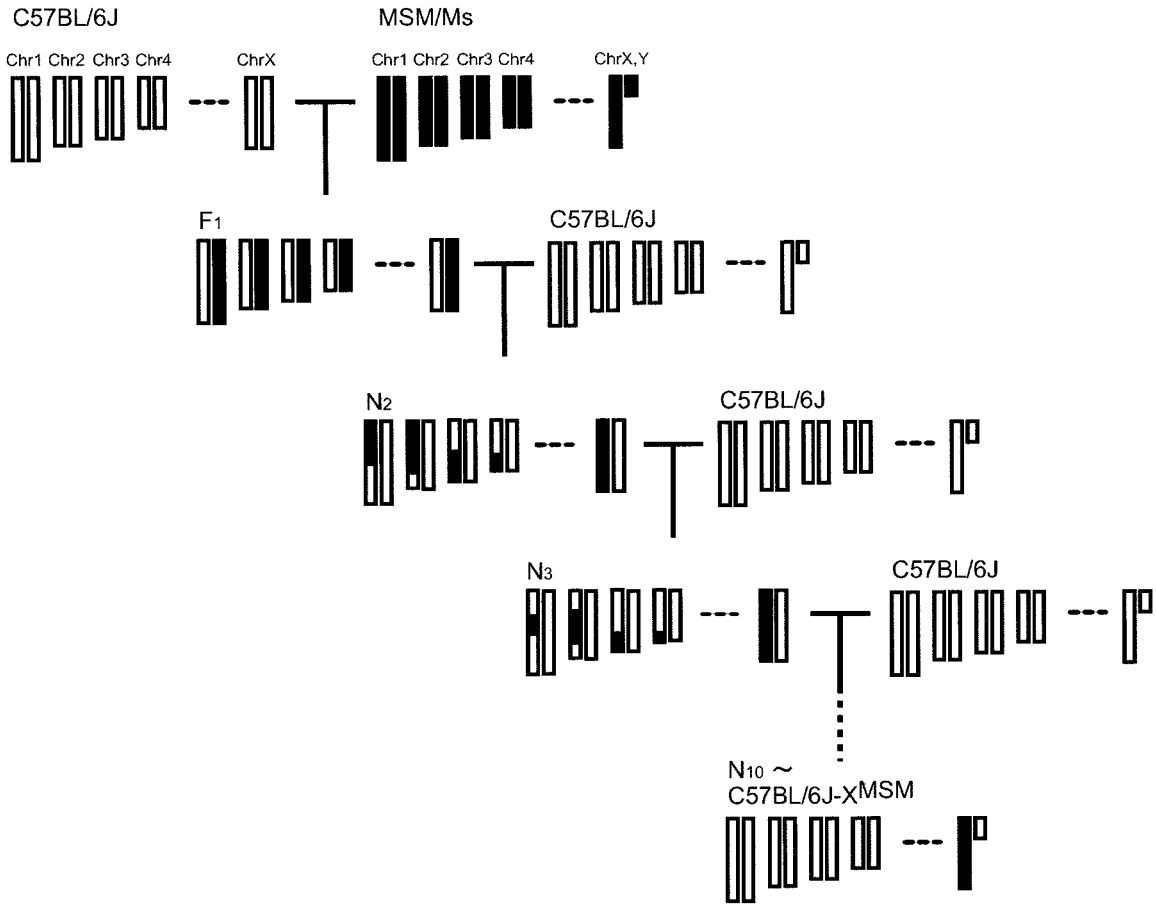


FIGURE 1.—Mating scheme to generate the X chromosomal consomic strain, C57BL/6J-$X^{MSM}$. (C57BL/6J × MSM/Ms) $F_1$ females were backcrossed to C57BL/6J males. For each subsequent backcross generation, female progeny with a nonrecombinant X chromosome from the MSM/Ms strain were selected by genotyping of 10 MIT microsatellite markers on the X chromosome; these females were backcrossed to C57BL/6J males. These backcrosses were repeated for >10 generations. The first backcross generation is designated $N_2$; subsequent backcross generations are designated $N_3$, etc.

Their average testis weight, however, was reduced to 62% of that of the B6-$X^{B6}$Y males. Other reproductive organs appeared normal. Histological analysis of the testes from the B6-$X^{MSM}$Y males of the $N_8$ revealed ongoing spermatogenesis, but there were various degrees of degeneration in the seminiferous tubules (Figure 2). In the most extreme case, the degenerated seminiferous tubules had thin and irregular epithelia, and developing spermatocytes and spermatids were sloughing into the lumen. It was also observed that a small number of

**TABLE 1**

**Reduction of fecundity of B6-$X^{MSM}$Y males**

| Males | Generation (no. of tested males) | No. of mated females | No. of reproductive males | No. of pregnant females | Litter size per pregnant female[a] |
|---|---|---|---|---|---|
| C57BL/6J | (9) | 30 | 6 | 13 | 7.9 ± 1.7 |
| B6-$X^{B6}$Y | $N_{8-10}$ (11) | 33 | 9 | 17 | 7.5 ± 2.5 |
| (C57BL/6J × MSM/Ms) $F_1$ | $F_1$ (10) | 29 | 9 | 17 | 7.4 ± 1.2 |
| B6-$X^{MSM}$Y | $N_2$ (10) | 30 | 9 | 21 | 5.0 ± 1.8[b] |
| | $N_3$ (10) | 30 | 2 | 2 | 3.0 ± 0 |
| | $N_{8-10}$ (12) | 36 | 0 | 0 | 0 |

[a] Values represent the mean litter size ±SD.

[b] The litter sizes in this cross were significantly lower than those in the cross with C57BL/6J males by Student's *t*-test ($P = 0.0119$).

**TABLE 2**

**Fertilization rate in the cross with B6-X$^{B6}$Y and B6-X$^{MSM}$Y males of the $N_{7–8}$**

| Males | No. of males | Total no. of 1-cell oocytes | Total no. of 2-cell embryos | % fertilization, mean ± SD |
|---|---|---|---|---|
| B6-X$^{B6}$Y | 10 | 37 | 124 | 80.4 ± 19.4 |
| B6-X$^{MSM}$Y | 7 | 103 | 0 | 0 |

**TABLE 3**

**Testis weight of the B6-X$^{B6}$Y and B6-X$^{MSM}$Y males ($N_{5–7}$ generations)**

| Males | *n* | Body weight (g) | Testis weight (mg) |
|---|---|---|---|
| B6-X$^{B6}$Y | 11 | 27.5 ± 2.7 | 100.0 ± 7.7 |
| B6-X$^{MSM}$Y | 12 | 30.0 ± 2.2 | 62.4 ± 7.8 |

Body and testis weight values represent the means ± SD. Values of the body weight of B6-X$^{MSM}$Y males were not significantly different from those of B6-X$^{B6}$Y males by Student's *t*-test ($P = 0.08$). Values of the testis weight of B6-X$^{MSM}$Y males were significantly lower than those of B6-X$^{B6}$Y males by Student's *t*-test ($P < 0.01$).

spermatogonia and Sertoli cells were retained along the basal laminae (Figure 2D). Hyperplasia of Leydig cells was observed in the interstitial space adjacent to the severely degenerated tubules (Figure 2B). In the other seminiferous tubules, where spermatogenesis was taking place, the total number of germ cells of all types was decreased and disrupted array and fragile adhesion were seen between seminiferous epithelia (Figure 2C). The cauda epididymal laminae of the B6-X$^{B6}$Y males were filled with mature spermatozoa, while those of the B6-X$^{MSM}$Y males contained both mature spermatozoa and abnormally developing germ cells (Figure 2F). Defects of spermatogenesis were observed in testes of some of the B6-X$^{B6}$Y males, but in most cases the defect was much less severe than that in the B6-X$^{MSM}$Y males (data not shown).

We measured serum testosterone level of the B6-X$^{MSM}$Y males and the control males, because a high level of serum testosterone in the B6-X$^{MSM}$Y males was expected from the hyperplasia of Leydig cells, which produce testosterone. The average testosterone level of the B6-X$^{MSM}$Y males of the $N_6$ did not, however, differ from that of C57BL/6J and the B6-X$^{B6}$Y males (C57BL/6J, 1.8 ng/ml ± 2.5, $n = 5$; B6-X$^{B6}$Y, 1.0 ng/ml ± 1.7, $n = 5$; B6-X$^{MSM}$Y, 1.3 ng/ml ± 2.1, $n = 5$).

**Abnormal morphology of the B6-X$^{MSM}$Y spermatozoa:** Sperm heads from the C57BL/6J males had, as expected, a falciform morphology with an extremely long apical hook (Figure 3A). Spermatozoa from (C57BL/6J × MSM/Ms) $F_1$ males also displayed normal morphology. In contrast, the B6-X$^{MSM}$Y males of the $N_2$ exhibited a slightly shortened distal region of the sperm heads. Sperm head malformations became much more severe after the $N_3$ (Figure 3C). In the extreme case, the apical hook of the sperm head was lost, and the sperm head was small and round. The severity of the abnormality through the different backcross generations was well correlated with the defect in fecundity. The B6-X$^{B6}$Y spermatozoa had normal head morphology through the backcross generations (Figure 3B).

For quantification of the sperm head morphology, sperm head morphologies were classified into the following six types as shown in Figure 4. Type 1 sperm has normal morphology. Type 2 has a slightly shortened apical hook. Type 3 has a narrowed sperm head throughout its length in addition to the slightly shortened apical hook. Type 4 shows a severely shortened apical hook and a squared posterior region. Type 5 is characterized by a loss of apical hook in addition to the squared posterior region. Type 6 is characterized by a small, round sperm head. The severity of the abnormality increases from type 2 to type 6. More than 100 spermatozoa from each male were classified into the above six types, and the percentage of each type was calculated. In the B6-X$^{B6}$Y males, the majority of spermatozoa were classified as type 1 (87%, $n = 19$ mice). In contrast, in the B6-X$^{MSM}$Y males, most of the spermatozoa were classified as type 4 (71%, $n = 14$ mice), and normal spermatozoa were rarely found. To quantify the severity of morphological defects, we gave points, 0–5, for types 1–6 and obtained a net score for individual males by adding up the percentage of their spermatozoa belonging to each type multiplied by the corresponding point value. Higher scores thus denote more severe abnormalities. The average net scores of the B6-X$^{B6}$Y and the B6-X$^{MSM}$Y males were 20 and 326, respectively (B6-X$^{B6}$Y, $n = 19$ mice; B6-X$^{MSM}$Y, $n = 14$ mice).

Observation with TEM revealed that epididymal spermatozoa of the B6-X$^{B6}$Y males had regular, spindle-shaped sperm nuclei (Figure 3D). In contrast, most of the sperm nuclei of the B6-X$^{MSM}$Y males had irregular, enlarged, curved, and hook-shaped or mushroom-shaped figures (Figure 3, E and F). Chromatin condensation seemed to occur normally in the sperm nuclei of the B6-X$^{MSM}$Y males, because all of the chromatin became condensed and darkly stained.

**Other abnormal characteristics of the B6-X$^{MSM}$Y spermatozoa:** We characterized other aspects of the B6-X$^{MSM}$Y spermatozoa; the results are summarized in Table 4. First, we counted the number of spermatozoa in cauda epididymides. The B6-X$^{MSM}$Y males had 38% as many spermatozoa in cauda epididymides as the B6-X$^{B6}$Y males. To test oviduct sperm transport, we isolated and counted spermatozoa from uteri and oviducts after mating with males. The number of spermatozoa in uteri was significantly lower in females mated with the B6-X$^{MSM}$Y males than in those mated with the B6-X$^{B6}$Y

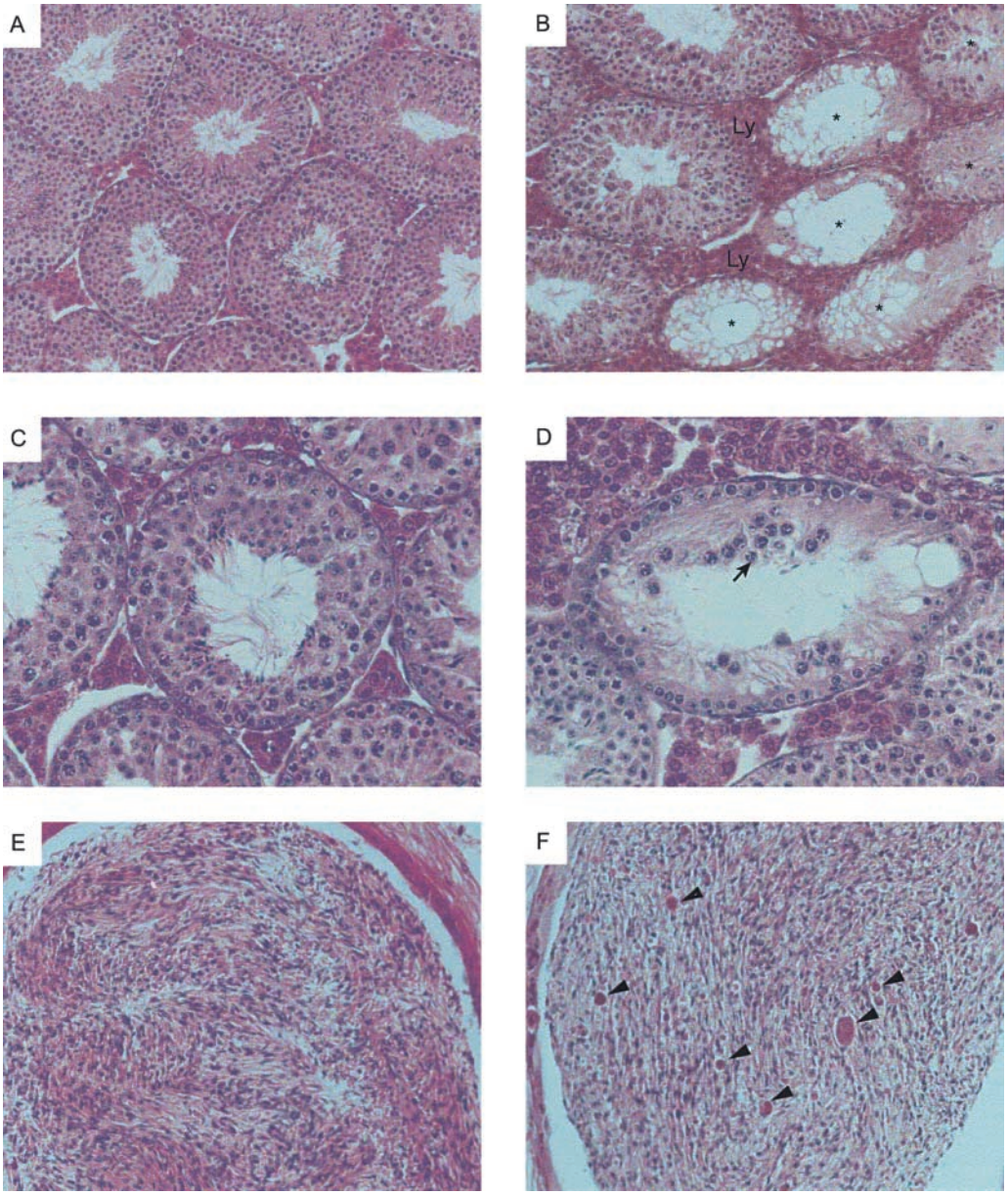


FIGURE 2.—Histological analyses of testes and cauda epididymides. (A and B) Sections of seminiferous tubules of C57BL/6J (A) mice and B6-$X^{MSM}Y$ (B) mice at $N_8$. The magnification is ×200. In the B6-$X^{MSM}Y$ males, seminiferous tubules were partially degenerated (*), and hyperplasia of Leydig cells (Ly) was observed in the interstitial spaces adjacent to disrupted tubules. (C and D) Spermatogenesis with moderate defects (C) and severe defects (D) was observed in the same B6-$X^{MSM}Y$ males. The magnification is ×400. Seminiferous tubules with moderate defects were characterized by thin and fragile epithelia with reduced numbers of germ cells. In severely degenerated tubules, only spermatogonia and Sertoli cells were observed, and pachytene spermatocytes (arrow) sloughing into the lumen were observed. (E and F) Cauda epididymis of the C57BL/6J (E) and B6-$X^{MSM}Y$ (F) males. The magnification is ×400. Differentiating spermatogenic cells (arrowheads) were observed as well as spermatozoa.

males. Spermatozoa in the oviducts showed a similar trend, although the difference was not statistically significant.

To assess the motility of spermatozoa, we incubated spermatozoa in medium and took hourly measurements of the SMI, which reflects both the concentration of motile spermatozoa and the extent of their motility (BARTOOV *et al.* 1991). The SMI values of both B6-$X^{B6}Y$ and B6-$X^{MSM}Y$ males showed typical temporal changes in sperm motility, in which the SMI values reached a peak after 2 hr in medium and then decreased gradually. The B6-$X^{B6}Y$ males exhibited normal SMI values, whereas the mean SMI value of the B6-$X^{MSM}Y$ males was significantly lower than that of the B6-$X^{B6}Y$ males at all time points.

Finally, we examined acrosome function of the B6-$X^{MSM}Y$ spermatozoa. Despite their abnormal sperm head morphology, the B6-$X^{MSM}Y$ spermatozoa displayed acrosomes. Moreover, the acrosome reaction of the spermatozoa was induced adequately when the spermatozoa were incubated with the calcium ionophore A23187, which induces the acrosome reaction.

**QTL analyses of X chromosomal factors responsible for reduced testis weight and sperm head abnormalities:** We conducted QTL analysis to map gene(s) on the X chromosome responsible for the reduced testis weight and the sperm head abnormality, using the Zmapqtl program of QTL Cartographer. We focused on these traits for the QTL analyses because they can be treated as quantitative traits, and the traits are likely related to the male sterility. For the analysis, data from 179 male progeny with recombinant or nonrecombinant X chromosomes generated from the $N_{5-7}$ backcrosses of the B6-$X^{MSM}X^{B6}$ heterozygous females to the C56BL/6J

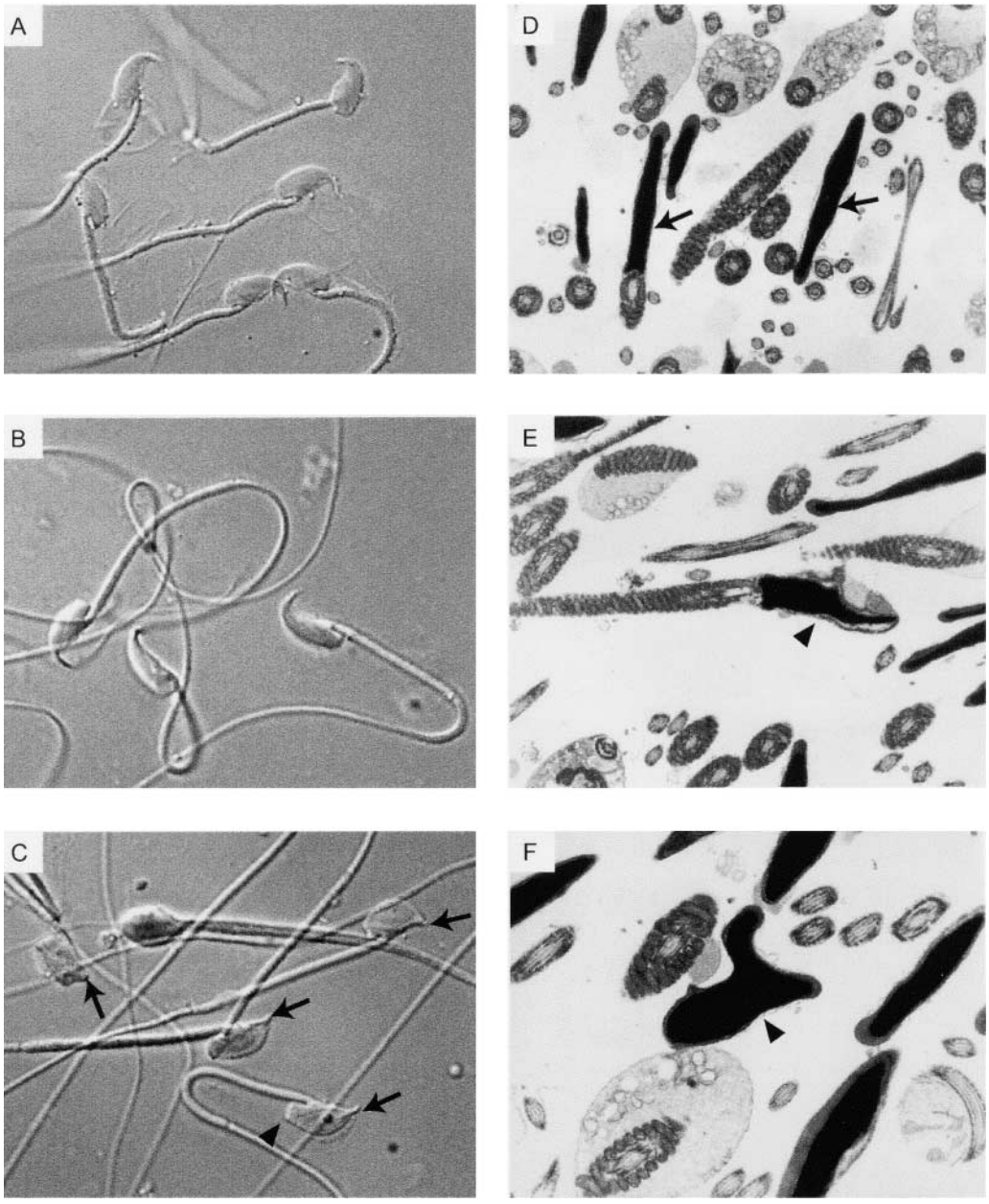


FIGURE 3.—Morphology of epididymal spermatozoa. (A–C) Light micrographs of spermatozoa from the C57BL/6J (A), B6-$X^{B6}Y$ (B), and B6-$X^{MSM}Y$ (C) males. The magnification is ×1000. Spermatozoa from the B6-$X^{MSM}Y$ male showed a shortened distal region (arrows) and squared posterior region (arrowhead) of sperm heads. (D–F) Transmission electron micrographs of spermatozoa from the B6-$X^{B6}Y$ (D) and the B6-$X^{MSM}Y$ (E and F) males. Spermatozoa from the B6-$X^{B6}Y$ males had regularly spindle-shaped nuclei (arrow). Abnormally shaped nuclei were observed in the B6-$X^{MSM}Y$ male (arrowhead). The magnification is ×5000 (D and E) or ×8000 (F).

males were compiled. Each male was genotyped using microsatellite markers described above and evaluated for the testis weight and the sperm head morphology. For the analysis of sperm head abnormality, a sperm head anomaly score for each male was used as a trait.

The testis weights of the progeny generated from the backcrosses showed a normal distribution ranging from 34.7 to 131.7 mg. The results of the QTL analysis are summarized in Figure 5A. The likelihood-ratio (LR) test statistic had a single peak, located at the distal region of the X chromosome between *DXMit97* and *DXMit249*. The maximum LR score of 110.7 lay in the interval between *DXMit4* and *DXMit217*, and the estimated additive effect was 14.7. In the model of this analysis, the difference between the mean phenotypic values of the B6-$X^{B6}Y$ and B6-$X^{MSM}Y$ males is represented by 2a. This QTL thus explains 78% of the difference in the average testis weights between the B6-$X^{B6}Y$ and B6-$X^{MSM}Y$ males.

We constructed a congenic strain that carries the MSM/Ms-derived X chromosome in the interval of *DXMit97–DXMit160* in the genetic background of the C57BL/6J strain. Males of this congenic strain showed partial disruption of spermatogenesis and their average testis weight was reduced to 69% of that of the B6-$X^{B6}Y$ males (the congenic strain, 69.2 mg ± 11.7, $n = 12$). Nevertheless, when each male was caged with three C57BL/6J females, six of seven males from the congenic strain produced progeny with litter sizes averaging 7.0 ± 1.6, which is normal as compared with that of the C57BL/6J males. The sperm morphology from these congenic males was normal (data not shown).

In the analysis of spermatozoa abnormality, the male

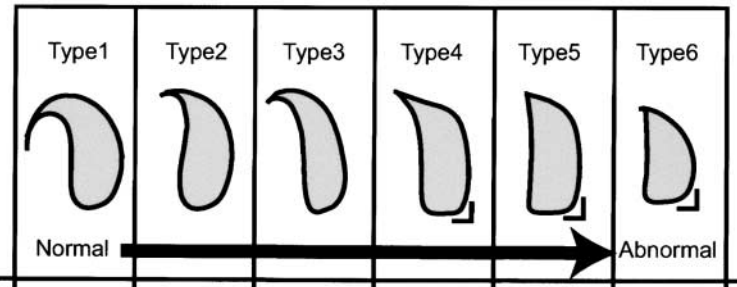


| Point / Males | 0 | 1 | 2 | 3 | 4 | 5 | Sperm head morphology score |
|---|---|---|---|---|---|---|---|
| B6-$X^{B6}Y$ (n = 19) | 87.0% | 8.4% | 3.1% | 1.3% | 0.2% | 0.1% | 19.8 |
| B6-$X^{MSM}Y$ (n = 14) | 0% | 4.0% | 1.6% | 71.0% | 13.3% | 10.6% | 326.2 |

FIGURE 4.—Quantification of morphological abnormalities of sperm heads. Sperm heads were classified into six types according to the severity of morphological defects. Type 1 is normal. The abnormality becomes more severe in types 2–6. The average frequency of each type in the B6-$X^{B6}Y$ and the B6-$X^{MSM}Y$ males is indicated in the boxes. The majority of spermatozoa from the B6-$X^{MSM}Y$ males at the $N_{5-7}$ were classified as type 4.

progeny of the $N_{5-7}$ backcross generations showed a distribution of sperm head morphology scores ranging from 0 to 394. The results of the QTL analysis for spermatozoa morphology are summarized in Figure 5B. The LR test statistic showed three peaks distributed across the X chromosome. The highest peak was located in the interval between *DXMit50* and *DXMit147*, the secondary one between *DXMit95* and *DXMit249*, and the lowest one between *DXMit89* and *DXMit50*. The maximum LR score of 110.1 lay in the interval between *DXMit144* and *DXMit109*, and the estimated additive effect was 71.4. This QTL explains 47% of the difference in the average sperm head morphology score between the B6-$X^{B6}Y$ and B6-$X^{MSM}Y$ males. The maximum LR scores in the other two peaks were 59.0 at 8.8 cM and 82.3 at 55.0 cM, respectively. The former QTL explains 35% and the latter explains 40% of the difference. We refer to the most proximal QTL between *DXMit89* and *DXMit50* as *s*perm *h*ead *a*nomaly *1* (*Sha1*), the QTL between *DXMit50* and *DXMit147* as *Sha2,* and the QTL between *DXMit95* and *DXMit*249 as *Sha3*. We searched for epistatic interactions among *Sha*s using the MImapqtl program of QTL Cartographer. The program detected a weak but significant epistatic interaction between *Sha1* and *Sha3* (data not shown).

## DISCUSSION

Hybrid sterility and hybrid breakdown are representative forms of postmating reproductive isolation. Study of reproductive isolation is crucial to understand the initiation of speciation. In this study, we reported a typical hybrid breakdown observed in interbreeding between C57BL/6J and MSM/Ms strains. It is notable that the $F_1$ hybrids of these two strains did not show any kind of reproductive abnormality.

It has been inferred that the majority of the C57BL/6J genome is derived from a Western European subspecies group, probably *M. m. domesticus*, which is genetically diverged by 1 million years from Asian wild mice, both the *musculus* subspecies group and the *castaneus* subspecies group (YONEKAWA *et al.* 1980; MORIWAKI 1994; KIKKAWA *et al.* 2001). Recent genome analysis based on single-nucleotide polymorphisms clearly indicated that the genomes of most standard laboratory inbred strains, including C57BL/6J, are mosaics of different subspecies groups from Europe and Asia. It is estimated that Asian mice contributed 21% of the genomes of the laboratory inbred strains (WADE *et al.* 2002). Japanese wild mice, *M. m. molossinus*, from which the MSM/Ms strain was established, originated mostly from the Asian *musculus* subspecies group and in part from the Asian *castaneus* subspecies group (YONEKAWA *et al.* 1980). Therefore, the C57BL/6J and MSM/Ms strains are genetically diverged in the majority of their genomes, and thus the hybrid breakdown observed in this study is attributable to intersubspecific differences in these two mouse strains.

This study demonstrated that males of the X chromosomal consomic strain, C57BL/6J-$X^{MSM}Y$, have reduced fecundity. This is a straightforward indication that the reduced fecundity results from incompatibility between the MSM/Ms alleles of one or more X chromosomal loci and C57BL/6J alleles of loci located on autosomes and/or the Y chromosome and thus that hybrid breakdown is caused by disruption of the interactions between

**TABLE 4**

**Characterization of spermatozoa from B6-X$^{B6}$Y and B6-X$^{MSM}$Y mice of $N_{5-7}$**

| Parameter | Males | | $n^b$ | $P$ |
|---|---|---|---|---|
| | B6-X$^{B6}$Y$^a$ | B6-X$^{MSM}$Y$^a$ | | |
| No. of spermatozoa in: | | | | |
| Epididymides ($\times 10^7$) | 3.3 ± 0.4 | 1.3 ± 0.6 | 3 | <0.01 |
| Uteri ($\times 10^4$) | 12.9 (2.2–22.3) | 3.4 (0.4–7.8) | 7 | 0.02 |
| Oviducts | 871.2 (92–2200) | 85.3 (12–264) | 6 | 0.10 |
| Sperm motility index (hr incubation) | | | | |
| 1 | 185.4 ± 59.2 | 84.2 ± 17.5 | 5–6 | <0.01 |
| 2 | 200.6 ± 32.4 | 88.3 ± 20.4 | 5–6 | <0.01 |
| 3 | 196.8 ± 48.2 | 83.3 ± 21.5 | 5–6 | <0.01 |
| 4 | 170.8 ± 49.1 | 72.8 ± 22.1 | 5–6 | <0.01 |
| % acrosome reaction | | | | |
| Medium only | 42.3 ± 11.5 | 44.1 ± 22.7 | 5 | 0.88 |
| Ionophore (min incubation) | | | | |
| 0 | 39.6 ± 8.4 | 43.5 ± 20.3 | 5 | 0.70 |
| 60 | 79.8 ± 6.2 | 82.6 ± 4.9 | 5 | 0.46 |
| 90 | 89.1 ± 4.0 | 89.0 ± 2.7 | 5 | 0.98 |

*P* values were determined by Student's *t*-test or Welch's *t*-test.
[a] Values represent the means ±SD or the means (range).
[b] Number of tested males.

these genes. It is noteworthy that the consomic females with the X$^{MSM}$X$^{B6}$ chromosome are fertile and that XO females with an MSM/Ms-derived X chromosome in the hybrid genetic background of C57BL/6 and CBA strains showed fertility even after the $N_5$ generation (Takagi *et al.* 1994). All these facts indicate that the hybrid breakdown involving the X$^{MSM}$ chromosome is male specific. In most cases, the reproductive isolation is first observed in the heterogametic sex (Haldane 1922). It has been also generally accepted that deleterious epistatic interactions between X-linked gene(s) and other chromosomal gene(s) would affect the sexes differentially (Muller 1940). Our observation is consistent with these theories.

In general, it is assumed that multiple genes are involved in hybrid breakdown. In this study, fecundity of the B6-X$^{MSM}$Y males declined rapidly in the early backcross generations, from the $N_2$ to $N_3$. This fact may imply that only a modest number of genes on autosomes and/or the Y chromosome, probably two or three, have interactions of major importance to male fecundity with X chromosomal genes. Future analysis using crosses of the C57BL/6J-X$^{MSM}$ strain with strains consomic for other chromosomes will answer the question as to which chromosomes interact with the X-linked gene(s).

The phenomenon of hybrid breakdown is of great use in investigating genetic interactions that underlie proper spermatogenesis. In-depth characterization of the sterile B6-X$^{MSM}$Y males revealed that they made copulation plugs at the normal rate, indicating normal mating behavior. Because no two-cell-stage embryos could be recovered from females mated with the B6-X$^{MSM}$Y males, the loss of fecundity is mainly due to the failure of fertilization. The B6-X$^{MSM}$Y males displayed reduced testis weight and moderate defects in spermatogenesis; in addition, we observed a significant reduction in the number of spermatozoa ejaculated by the B6-X$^{MSM}$Y males that reached the female reproductive tracts. This contributes, in part, to the sterility of the B6-X$^{MSM}$Y males. More strikingly, the B6-X$^{MSM}$Y spermatozoa had severely abnormal morphology, with shortened apical hooks, although the spermatozoa induced adequate acrosome reactions. Moreover, we found that the motility of the B6-X$^{MSM}$Y spermatozoa was significantly lower than that of the control B6-X$^{B6}$Y spermatozoa. Taken together, these results imply that the impaired fertility of the B6-X$^{MSM}$Y males is probably due to failure of the spermatozoa to reach unfertilized oocytes in ampulla and/or failure to penetrate into the cumulus layer or zona pellucida, possibly because of the lower motility and the misshapen heads of the spermatozoa.

QTL analysis revealed a single major region responsible for the reduced testis weight of B6-X$^{MSM}$Y males; this locus is in an interval between *DXMit97* and *DXMit249* in the distal region of the X chromosome. A congenic strain that carries this critical region from the MSM/Ms strain in the genetic background of the C57BL/6J strain displayed reduced testis weight, confirming the importance of this region. Previous studies showed re-

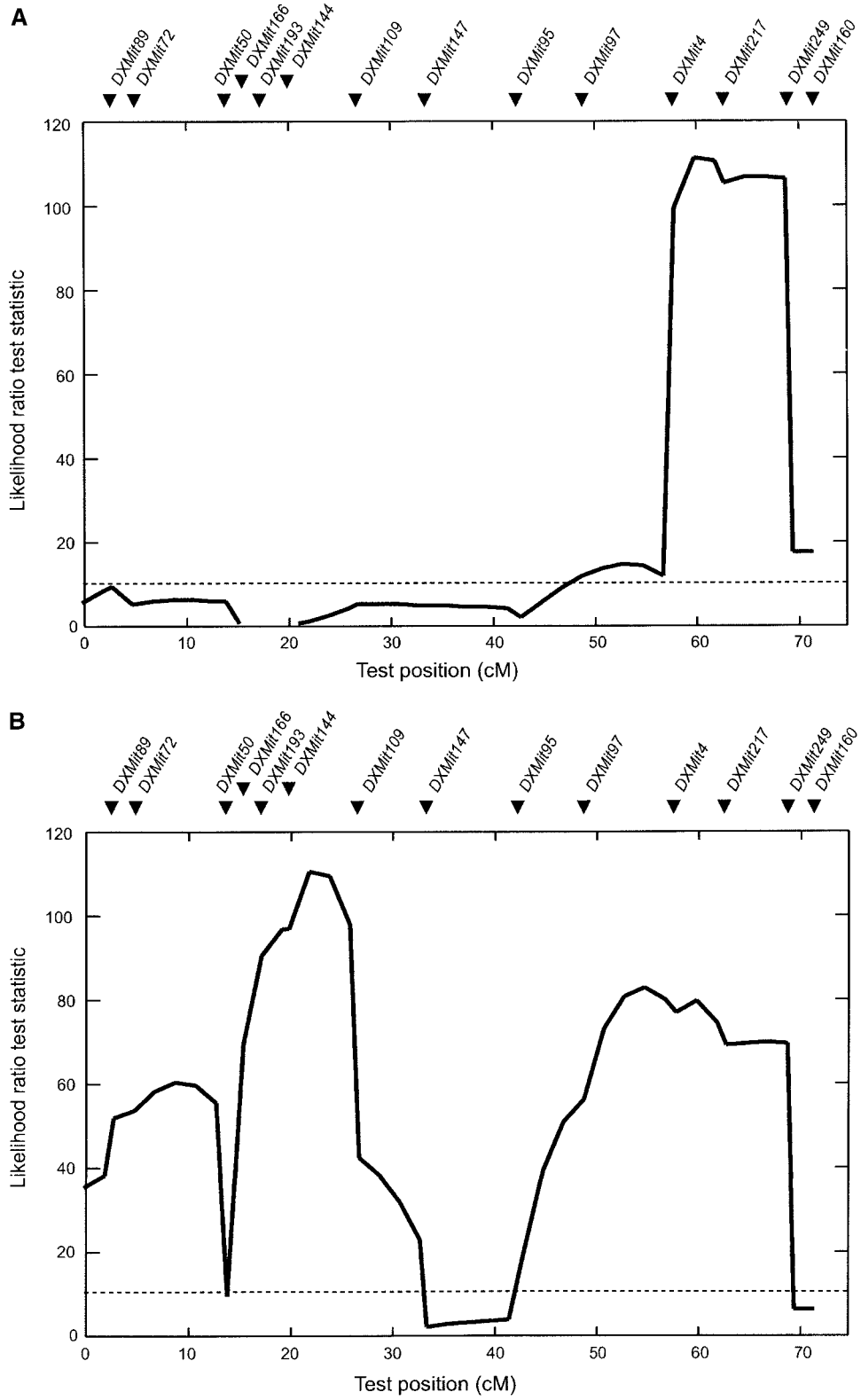


FIGURE 5.—Result of QTL analysis for testis weight (A) and sperm head morphology (B), using data compiled from all the male progeny of the $N_{5-7}$ from crosses of the B6-$X^{MSM}X^{B6}$ females and the C57BL/6J males. The likelihood-ratio test statistic is plotted at 1-cM intervals. The 5% critical value is indicated by a dotted line.

duced testis weight and dissociation of X and Y chromosomes during male meiosis in intersubspecific and interspecific $F_1$ hybrids (MATSUDA *et al.* 1982, 1991; GUÉNET *et al.* 1990). It was proposed that the hybrid sterility and the reduced testis weight are caused by structural incompatibility between the pseudo-autosomal regions of X and Y chromosomes. The boundary of the pseudo-autosomal region is located between *DXMit249* and

*DXMit160* in the C57BL/6J strain (Perry *et al.* 2001). Thus, the QTL for the testis weight, which we mapped between *DXMit97* and *DXMit249*, is probably outside the pseudo-autosomal region and not related to the reported hybrid sterility. In fact, we found that the congenic males carrying the MSM/Ms-derived chromosomal segment between *DXMit97* and *DXMit249* were fertile and that they produced normal spermatozoa. Thus, although the distal region of the X chromosome may contribute to the process of spermatogenesis, it is clear that the sterility of the B6-$X^{MSM}Y$ males is not caused directly by the reduced testis weight.

QTL analysis for the sperm head abnormality indicated three candidate loci. Among them, a major peak we refer to as *Sha2* is located in the central region of the X chromosome. Previous mapping of the X-linked gene responsible for the hybrid breakdown identified *Shx1*, a locus 29 cM from the centromere, on the basis of a relatively small number of progeny of crosses involving XO females (Takagi *et al.* 1994). *Shx1* is close to *Sha2* detected in this study. This region contains several candidate genes that are expressed in testes. They include haploid-specific alanine-rich protein located on chromosome X (*Halap-X*; Uchida *et al.* 2000); nuclear receptor subfamily 0, group B member 1 (*Nr0b1*); androgen receptor (*AR*); fragile-X mental retardation syndrome 1 homolog (*Fmr1*); and SRY-box-containing gene 3 (*Sox3*). Sequencing of *Halap-X, NrOb1*, and *AR* indicated nonsynonymous substitutions between C57BL/6J and MSM/Ms alleles, but not of *Fmr1* and *Sox3*.

The transformation of spermatids to spermatozoa includes a complex sequence of events: formation of the acrosome, nuclear changes, development of the flagellum, reorganization of the cytoplasm and cell organelles, and elimination of residual bodies by Sertoli cells. Little is known about the molecular mechanisms underlying such dynamic changes of the sperm head morphology. The primary defect in the B6-$X^{MSM}Y$ males is abnormality of anterior head shape of the spermatozoa, suggesting that the *Sha* genes might play key roles in sperm head morphogenesis. Identification of the *Sha* genes on the X chromosomes and of the interacting gene(s) located on autosomes and/or the Y chromosome would provide insight into this problem. The results of this study imply that genes involved in sperm head morphogenesis may be responsible for the male sterility in hybrid breakdown, because the reduction in fecundity was correlated with the severity of the abnormalities of the sperm head morphology through the backcross generations. In this context, it is interesting to note that the shape of spermatozoa varies enormously across and among species. Therefore, it is most likely that the morphological diversification is largely related to postmating isolation during the evolutionary process.

Male infertility accounts for 5–7% of infertility in human couples (Cooke and Sauners 2002). Abnormal shape of spermatozoa is a common feature of human male infertility. So far, detailed investigation of the causes of infertility has relied on studies with mutant mice. Mutational disorders are responsible for some cases of male infertility, but the causes of many cases are still unknown. Genetic incompatibilities may also contribute to human male infertility. The use of the mouse consomic strains as a model system may shed light on genetic aspects of human infertility.

We thank H. Yonekawa, Y. Kikkawa, and Y. Mizushina for useful discussion and comments on this work and K. Hiratsuka and M. Arii for maintenance of mice. This research was supported in part by the "Genome Frontier Development Promotion" assisted by the Special Coordination Funds for Promoting and Science and Technology of the Ministry of Education, Culture, Sports, Science, and Technology of Japan and in part by grants in aid from the Ministry of Education, Culture, Sports, Science, and Technology of Japan. This article is contribution no. 2497 from the National Institute of Genetics, Japan.

## LITERATURE CITED

Bartoov, B., A. Mayevsky, M. Sneider, L. Yogev and A. Lightman, 1991 Sperm motility index: a new parameter for human sperm evaluation. Fertil. Steril. **56:** 108–112.

Basten, C. J., B. S. Weir and Z-B. Zeng, 1997 *QTL Cartographer: A Reference Manual and Tutorial for QTL Mapping*. Department of Statistics, North Carolina State University, Raleigh, NC.

Bonhomme, F., and J-L. Guénet, 1996 The laboratory mouse and its wild relatives, pp. 1577–1596 in *Genetic Variations and Strains of the Laboratory Mouse*, edited by M. F. Lyon, S. Rastan and M. Brown. Oxford University Press, London/New York/Oxford.

Bonhomme, F., J-L. Guénet, B. Dod, K. Moriwaki and G. Bulfield, 1987 The polyphyletic origin of laboratory inbred mice and their rate of evolution. Biol. J. Linn. Soc. **30:** 51–58.

Cooke, H. J., and P. T. K. Sauners, 2002 Mouse models of males infertility. Nat. Rev. Genet. **3:** 790–801.

Didion, B. A., J. R. Dobrinsky, J. R. Giles and C. N. Graves, 1989 Staining procedure to detect viability and the true acrosome reaction in spermatozoa of various species. Gamete Res. **22:** 51–57.

Elliott, R. W., D. R. Miller, R. S. Pearsall, C. Hohman, Y. Zhang *et al.*, 2001 Genetic analysis of testis weight and fertility in an interspecies hybrid congenic strain for chromosome X. Mamm. Genome **12:** 45–51.

Forejt, J., and P. Ivanyi, 1975 Genetic studies on male sterility of hybrids between laboratory and wild mouse (*Mus musculus* L.). Genet. Res. **24:** 189–206.

Forejt, J., V. Vincek, J. Klein, H. Lehrach and M. Loudove-Michova, 1991 Genetic mapping of the *t*-complex region on mouse chromosome 17 including the hybrid sterility-1 gene. Mamm. Genome **1:** 84–91.

Guénet, J-L., C. Nagamine, D. Simon-Chazottes, X. Montagutelli and F. Bonhomme, 1990 *Hst-3*, an X-linked hybrid sterility gene. Genet. Res. **56:** 163–165.

Haldane, J. B. S., 1922 Sex ratio and unisexual sterility in hybrid animals. J. Genet. **12:** 101–109.

Kikkawa, Y., I. Miura, S. Takahama, S. Wakana, Y. Yamazaki *et al.*, 2001 Microsatellite database for MSM/Ms and JF1/Ms, *molossinus*-derived strains. Mamm. Genome **12:** 750–752.

Matsuda, Y., H. T. Imai, K. Moriwaki, K. Kondo and F. Bonhomme, 1982 X-Y chromosome dissociation in wild derived *M. musculus* subspecies, laboratory mice, and their F1 hybrids. Cytogenet. Cell Genet. **34:** 241–252.

Matsuda, Y., T. Hirobe and V. M. Chapman, 1991 Genetic basis of X-Y chromosome dissociation and male sterility in interspecific hybrids. Proc. Natl. Acad. Sci. USA **88:** 4850–4854.

Moriwaki, K., 1994 Wild mice from the geneticist's viewpoint, pp. xiii–xxv in *Genetics in Wild Mice: Its Application to Biomedical Research*, edited by K. Moriwaki, T. Shiroishi and H. Yonekawa. Japan Scientific Press/Karger, Tokyo.

Muller, H. J., 1940 Bearing of the Drosophila work on systematics,

pp. 185–268 in *The New Systematics*, edited by J. Huxley. Clarendon Press, Oxford.

Nadeau, J. H., J. B. Singer, A. Matin and E. S. Lander, 2000 Analysing complex genetic traits with chromosome substitution strains. Nat. Genet. **24:** 221–225.

Orr, H. A., 1993 Haldane's rule has multiple genetic causes. Nature **361:** 532–533.

Perry, J., S. Palmer, A. Gabriel and A. Ashworth, 2001 A short pseudoautosomal region in laboratory mice. Genome Res. **11:** 1826–1832.

Pilder, S. H., 1997 Identification and linkage mapping of *Hst7*, a new *M. spretus/M. m. domesticus* chromosome 17 hybrid sterility locus. Mamm. Genome **8:** 290–303.

Pilder, S. H., M. F. Hammer and L. M. Silver, 1991 A novel mouse chromosome 17 hybrid sterility locus: implications for the origin of *t* haplotypes. Genetics **129:** 237–246.

Pilder, S. H., P. Olds-Clarke, D. M. Philips and L. M. Silver, 1993 Hybrid sterility-6: a mouse *t* complex locus controlling sperm flagellar assembly and movement. Dev. Biol. **159:** 631–642.

Pilder, S. H., P. Olds-Clarke, J. M. Orth, W. F. Jester and L. Dugan, 1997 Hst7: a male sterility mutation perturbing sperm motility, flagellar assembly, and mitochondrial sheath differentiation. J. Androl. **18:** 663–671.

Takagi, N., M. Tada, M. Shoji and K. Moriwaki, 1994 An X-linked gene governing sperm morphology revealed in laboratory mice consomic for X chromosome from Japanese house mouse, *M. musculus molossinus*, pp. 247–256 in *Genetics in Wild Mice: Its Application to Biomedical Research*, edited by K. Moriwaki, T. Shiroishi and H. Yonekawa. Japan Scientific Press/Karger, Tokyo.

Toshimori, K., and C. Oura, 1993 Fine structural changes in the postacrosomal region of the hamster and mouse sperm head at the initial stages of gamete interaction. Arch. Histol. Cytol. **56:** 109–116.

Toyoda, Y., M. Yokoyama and T. Hoshi, 1971 Studies on the fertilization of mouse eggs *in vitro*. Jpn. J. Anim. Reprod. **16:** 147–157.

Trachtulec, Z., M. Mnulova-Fajdelova, R. M. J. Hamvas, S. Gregorova, W. E. Mayer *et al.*, 1997 Isolation of candidate hybrid sterility 1 genes by cDNA selection in a 1.1 megabase pair region on mouse chromosome 17. Mamm. Genome **8:** 312–316.

Uchida, K., J. Tsuchida, H. Tanaka, M. Koga, Y. Nishina *et al.*, 2000 Cloning and characterization of a complementary deoxyribonucleic acid encoding haploid-specific alanine-rich acidic protein located on chromosome-X. Biol. Reprod. **63:** 993–999.

Wade, C. M., E. J. Kulbokas, III, A. W. Kirby, M. C. Zody, J. C. Mullikin *et al.*, 2002 The mosaic structure of variation in the laboratory mouse genome. Nature **420:** 564–578.

Whittingham, D. G., S. P. Leibo and P. Mazur, 1972 Survival of mouse embryos frozen to −109° and −269° C. Science **178:** 411–414.

Yonekawa, H., K. Moriwaki, O. Gotoh, J.-I. Hayashi, J. Watanabe *et al.*, 1980 Relationship between laboratory mice and subspecies *Mus musculus domesticus* based on restriction endonuclease cleavage patterns of mitochondria DNA. Jpn. J. Genet. **55:** 289–296.

Zeng, Z-B., 1993 Theoretical basis for separation of multiple linked gene effects in mapping quantitative trait loci. Proc. Natl. Acad. Sci. USA **90:** 10972–10976.

Zeng, Z-B., 1994 Precision mapping of quantitative trait loci. Genetics **136:** 1457–1468.

Communicating editor: C. Kozak